Cotunneling Current and Shot Noise in Quantum Dots

Axel Thielmann,[1] Matthias H. Hettler,[1] Jürgen König,[2] and Gerd Schön[1,3]

[1]*Forschungszentrum Karlsruhe, Institut für Nanotechnologie, 76021 Karlsruhe, Germany*
[2]*Institut für Theoretische Physik III, Ruhr-Universität Bochum, 44780 Bochum, Germany*
[3]*Institut für Theoretische Festkörperphysik, Universität Karlsruhe, 76128 Karlsruhe, Germany*

(Received 21 January 2005; published 30 September 2005)

We derive general expressions for the current and the shot noise, taking into account non-Markovian memory effects. In generalization of previous approaches, our theory is valid for an arbitrary Coulomb interaction and coupling strength and is applicable to quantum dots and more complex systems such as molecules. A fully consistent diagrammatic expansion up to second order in the coupling strength, taking into account cotunneling processes, allows for a study of transport in an intermediate coupling strength regime relevant to many current experiments. We discuss a single-level quantum dot as a first example, focusing on the Coulomb-blockade regime where the cotunneling processes dominate. We find super-Poissonian shot noise due to inelastic spin-flip cotunneling processes at an energy scale different from the one expected from first-order calculations.

DOI: 10.1103/PhysRevLett.95.146806 PACS numbers: 73.63.−b, 72.70.+m, 73.23.Hk

Introduction.—The study of shot noise in transport through mesoscopic devices, such as quantum dots or molecular devices, is a field of intense theoretical and experimental research [1]. It provides additional information, not contained in the current, about system parameters that govern the electronic transport [2]. For weak coupling between the quantum dot and metallic electrodes, transport is dominated by sequential tunneling [3], described by first-order perturbation theory in the coupling strength Γ, or its variants to include coherence effects [4]. Shot noise in this limit has been studied for a variety of models, including effects from electronic interactions [2–4], generalizations to multilevel dots, allowing for coupling to photonic and vibrational modes [2,5,6], or spin-polarized leads [7]. However, a theory taking fully into account interaction effects as well as arbitrary coupling strength does not exist. Expressions for the shot noise in terms of nonequilibrium Green functions have been derived only in the absence of Coulomb interactions or in a perturbative expansion thereof [8].

Shot noise has been measured in various experimental realizations [9–11]. As the strength of the coupling in a given experiment is not *a priori* known, it is unclear whether first-order calculations are sufficient. Second order tunneling (cotunneling [12]) processes can play an important role for the conductance [13], particularly in the Coulomb-blockade regime. Shot noise in this regime has been discussed theoretically in Ref. [14] where the possibility of super-Poissonian noise was suggested. However, that work was limited to pure cotunneling processes, which is inadequate for the experiment of Ref. [13].

In this Letter we provide a complete description of the current and shot noise, valid for arbitrary coupling strength Γ, while accounting fully for the Coulomb interaction. By making use of a diagrammatic language, we expand the expressions up to second order in our only perturbative parameter, the ratio of the coupling strength to the temperature, $\Gamma/k_{\mathrm{B}}T$. We study explicitly the example of a single-level quantum dot, out of equilibrium for any bias voltage. The theory covers the Coulomb-blockade regime (low bias), the sequential-tunneling regime (bias larger than the first single-charge excitation energy), and the crossover between both. We find that super-Poissonian shot noise appears in the Coulomb-blockade regime due to the inelastic spin-flip cotunneling processes. This occurs at a different energy scale than expected from first-order calculations. We also show that the noise to current ratio is highly sensitive to the coupling strength in this regime. This may serve as an additional spectroscopic tool for the couplings.

The model.—The Anderson-impurity model is based on the Hamiltonian $\hat{H} = \hat{H}_{\mathrm{L}} + \hat{H}_{\mathrm{R}} + \hat{H}_{\mathrm{dot}} + \hat{H}_{\mathrm{T,L}} + \hat{H}_{\mathrm{T,R}}$ with $\hat{H}_r = \sum_{k\sigma} \epsilon_{k\sigma r} a^\dagger_{k\sigma r} a_{k\sigma r}$, $\hat{H}_{\mathrm{dot}} = \sum_\sigma \epsilon_\sigma c^\dagger_\sigma c_\sigma + U n_\uparrow n_\downarrow$ and $\hat{H}_{\mathrm{T},r} = \sum_{k\sigma} (t_r a^\dagger_{k\sigma r} c_\sigma + \mathrm{H.c.})$ for $r = \mathrm{L}, \mathrm{R}$. Here, $\hat{H}_{\mathrm{L}}$ and $\hat{H}_{\mathrm{R}}$ describe the left and right electrodes with noninteracting electrons, $\hat{H}_{\mathrm{dot}}$ the quantum dot with one (spin-dependent) level of energy ϵ_σ, and Coulomb interaction U for double occupancy of the dot. Tunneling between the leads and the dot is modeled by $\hat{H}_{\mathrm{T,L}}$ and $\hat{H}_{\mathrm{T,R}}$. The coupling strength is characterized by the intrinsic line width $\Gamma_r = 2\pi\rho_e |t_r|^2$, where ρ_e is the (constant) density of states of the leads. For later use we define $\Gamma = \Gamma_{\mathrm{L}} + \Gamma_{\mathrm{R}}$. The creation and annihilation operators $a^\dagger_{k\sigma r}(a_{k\sigma r})$ and $c^\dagger_\sigma(c_\sigma)$ refer to the electrodes and the dot, and $n_\sigma = c^\dagger_\sigma c_\sigma$.

We are interested in the current I and the (zero-frequency) current noise S, which for $eV \gg k_{\mathrm{B}}T$ is dominated by shot noise. Both quantities are related to the (symmetrized) current operator $\hat{I} = (\hat{I}_{\mathrm{R}} - \hat{I}_{\mathrm{L}})/2$ with $\hat{I}_r = -i(e/\hbar)\sum_{k\sigma}(t_r a^\dagger_{k\sigma r} c_\sigma - \mathrm{H.c.})$, from which we obtain $I = \langle \hat{I} \rangle$ and

$$S = 2 \int_{-\infty}^{0} dt [\langle \hat{I}(t)\hat{I}(0) + \hat{I}(0)\hat{I}(t) \rangle - 2\langle \hat{I} \rangle^2]. \qquad (1)$$

Diagrammatic technique.—In Ref. [2] we have formulated a theory of current noise for transport to first order in Γ, based on a diagrammatic language that has been developed for a systematic perturbation expansion of the current through localized levels [15]. All transport properties are governed by the nonequilibrium time evolution of the density matrix. The electrode degrees of freedom can be integrated out, and we obtain a reduced density matrix for the dot degrees of freedom only, labeled by χ. The time evolution of the reduced density matrix, described by the propagator $\Pi_{\chi'\chi}(t', t)$ for the propagation from a state χ at time t to a state χ' at time t', can be visualized by diagrams [2,15] on the Keldysh contour. The full propagation is expressed as a sequence of irreducible blocks (self-energies) $W_{\chi'\chi}(t', t)$ that are associated with transitions from state χ at time t to state χ' at time t'. This yields the Dyson equation

$$\mathbf{\Pi}(t', t) = \mathbf{1} + \int_t^{t'} dt_2 \int_t^{t_2} dt_1 \mathbf{W}(t_2, t_1)\mathbf{\Pi}(t_1, t) \qquad (2)$$

for the propagator, where the boldface indicates matrix notation related to the dot eigenstate labels. For the following, it is convenient to introduce the Laplace transform $\mathbf{W}(z) = \hbar \int_{-\infty}^{0} dt e^{zt} \mathbf{W}(0, t)$ and the definitions $\mathbf{W} = \mathbf{W}(z)|_{z=0^+}$ and $\partial\mathbf{W} = -(\partial\mathbf{W}(z)/\partial z)|_{z=0^+}$.

In the long-time limit, i.e., for time differences $t' - t$ larger than the correlation time ($\propto 1/\Gamma$) over which the system forgets its initial state, the propagator becomes $\mathbf{p}^{\rm st} \otimes \mathbf{e}^T$, where $\mathbf{e}^T = (1, 1, \ldots, 1)$, and $\mathbf{p}^{\rm st}$ is the vector of the stationary probabilities, determined from $\mathbf{W}\mathbf{p}^{\rm st} = \mathbf{0}$, independent of the initial (diagonal) density matrix. As $\mathbf{W}$ has a zero eigenvalue, it cannot be inverted. With the normalization condition $\mathbf{e}^T\mathbf{p}^{\rm st} = 1$ we obtain the stationary probabilities $\mathbf{p}^{\rm st}$ by solving

$$(\tilde{\mathbf{W}}\mathbf{p}^{\rm st})_\chi = \Gamma\delta_{\chi,\chi_0}, \qquad (3)$$

where $\tilde{\mathbf{W}}$ is identical to $\mathbf{W}$ but with one (arbitrarily chosen) row χ_0 being replaced with $(\Gamma, \ldots, \Gamma)$ [2].

For a diagrammatic representation of the current, we introduce a block $\mathbf{W}^I$, in which one (internal) tunneling vertex is replaced by an external vertex for the current operator $\hat{I}$ divided by $e/\hbar$. We get

$$I = \frac{e}{2\hbar}\mathbf{e}^T\mathbf{W}^I\mathbf{p}^{\rm st}. \qquad (4)$$

The shot noise, Eq. (1), involves expectation values of two current operators. They appear either in a single irreducible block, which we denote by $\mathbf{W}^{II}$, or in two different blocks $\mathbf{W}^I$. We find

$$S = \frac{e^2}{\hbar}\mathbf{e}^T[\mathbf{W}^{II} + \mathbf{W}^I(\mathbf{P}\mathbf{W}^I - \mathbf{p}^{\rm st} \otimes \mathbf{e}^T\partial\mathbf{W}^I)]\mathbf{p}^{\rm st} \qquad (5)$$

with $\partial\mathbf{W}^I = -(\partial\mathbf{W}^I(z)/\partial z)|_{z=0^+}$. The object $\mathbf{P} = \int_{-\infty}^{0} dt \frac{1}{\hbar}[\mathbf{\Pi}(0, t) - \mathbf{\Pi}(0, -\infty)]$ is determined by

$$\tilde{\mathbf{W}}\mathbf{P} = \partial\tilde{\mathbf{W}}\mathbf{p}^{\rm st} \otimes \mathbf{e}^T + (\mathbf{p}^{\rm st} \otimes \mathbf{e}^T - \mathbf{1})(\mathbf{1} - \delta_{\chi',\chi_0}), \qquad (6)$$

where we use the extra condition $\mathbf{e}^T\mathbf{P} = \mathbf{0}$, which follows from the definition of $\mathbf{P}$, the Dyson equation, and $\mathbf{e}^T\mathbf{W} = \mathbf{0}$. The set of matrix equations, Eqs. (3)–(6), constitutes the starting point for all results presented below. For a systematic perturbation expansion of current I and noise S in Γ, we expand all quantities $\tilde{\mathbf{W}}$, $\mathbf{W}^I$, $\mathbf{W}^{II}$, $\partial\mathbf{W}$, $\partial\mathbf{W}^I$, $\mathbf{p}^{\rm st}$, and $\mathbf{P}$ order by order. For transport in first order (sequential tunneling), the above expressions simplify, as all contributions involving the derivatives $\partial\mathbf{W}$ and $\partial\mathbf{W}^I$ disappear as a consequence of the fact that $\mathbf{W}$ starts at order Γ, $\mathbf{p}^{\rm st}$ at Γ^0, and $\mathbf{P}$ at Γ^{-1}. These derivatives are associated with non-Markovian behavior of the system and have not been taken into account in Refs. [2,3]. They are absent for first-order transport, but they are important for second- and higher-order corrections (for a discussion of non-Markovian effects see also Ref. [16]). Higher derivatives will not appear for the shot noise even for higher-order corrections.

We emphasize that the expressions derived above are valid for rather general Hamiltonians, such as arrays of quantum dots or small molecules with many levels and full two-body electron interactions [17,18]. In the following, however, we focus on the Anderson-impurity model.

Results.—We now recall the main features of first-order (sequential) transport. Both current and shot noise increase monotonically with bias voltage, and display plateaus separated by thermally broadened steps. The step positions are given by the energy parameters, which determine the bias needed to make single-charge excitations energetically possible. The coupling parameters set the plateau heights.

Higher-order transport modifies the current and noise in two different ways. First, it introduces an additional broadening of the steps; i.e., the latter is effectively given by the sum of Γ and T. Second, it allows for transport in the Coulomb-blockade region at low bias, where sequential tunneling is suppressed. With increasing coupling strength Γ, second-order and eventually also higher-order corrections to transport become more and more important. To illustrate the validity range of our second order perturbation expansion, we first consider the noninteracting limit, $U = 0$, since in this case exact results [1] are available for the current $I_{U=0} = e/h \int d\omega \sum_\sigma \tau_\sigma(\omega)[f_{\rm L}(\omega) - f_{\rm R}(\omega)]$ and shot noise $S_{U=0} = 2e^2/h \int d\omega \sum_\sigma \{\tau_\sigma(\omega) \times [f_{\rm L}(\omega) \times (1 - f_{\rm L}(\omega)) + f_{\rm R}(\omega)(1 - f_{\rm R}(\omega))] + \tau_\sigma(\omega) \times (1 - \tau_\sigma(\omega))[f_{\rm L}(\omega) - f_{\rm R}(\omega)]^2\}$ with $\tau_\sigma(\omega) = \Gamma_{\rm L}\Gamma_{\rm R}/[(\omega - \epsilon_\sigma)^2 + (\Gamma/2)^2]$. The result is shown in Fig. 1 where we compare first order, (first plus) second order, and exact current and noise for the parameter set $\epsilon_\downarrow = -1.5$ meV, $\epsilon_\uparrow = 0.5$ meV, $k_{\rm B}T = 0.1$ meV, and $\Gamma_{\rm L} = \Gamma_{\rm R} = \Gamma/2$. We choose a symmetric bias voltage, such that $\mu_{\rm L} = {\rm eV}/2$ and $\mu_{\rm R} = -{\rm eV}/2$. Outside the Coulomb-blockade regime, the second order corrections (dashed lines) to sequential tunneling (dotted lines) start to become important for $\Gamma/k_{\rm B}T < 0.5$. As long as $\Gamma/k_{\rm B}T < 1$, the exact curves (solid lines) are perfectly reproduced by second order perturbation theory, while the sequential-tunneling results clearly deviate. For $\Gamma/k_{\rm B}T = 2$ third-order contri-

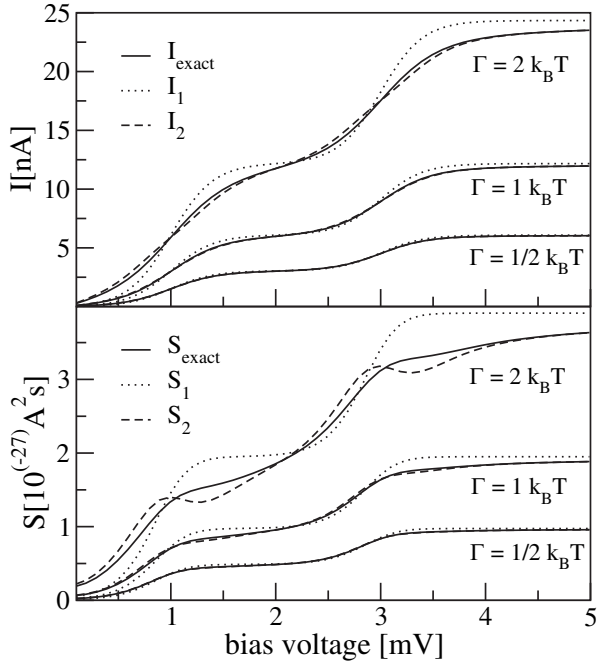

FIG. 1. Current I and shot noise S vs bias voltage for $k_BT = 0.1$ meV, $\epsilon_\downarrow = -1.5$ meV, $\epsilon_\uparrow = 0.5$ meV, $U = 0$, and $\Gamma_L = \Gamma_R = \Gamma/2$. First order (dotted lines) and second order (dashed lines) are compared to the exact results (solid lines) for $\Gamma/k_BT = 0.5, 1, 2$.

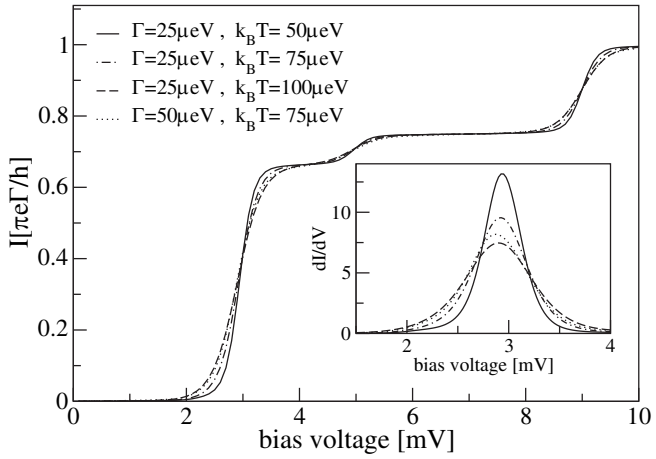

FIG. 2. Current I and conductance dI/dV (inset) vs bias voltage for $\epsilon_\downarrow = -1.5$ meV, $\epsilon_\uparrow = 0.5$ meV, $U = 4$ meV, and $\Gamma_L = \Gamma_R = \Gamma/2$ for various values of Γ and k_BT. The broadening of the first step due to Γ and k_BT is shown in the inset. The dashed and dotted curves with the same $(\Gamma + k_BT)$ have about the same width.

butions start to play a role, at least for the noise, where unphysical nonmonotonicities arise around the steps. We, therefore, restrict ourselves to $\Gamma \leq k_BT$ for the following discussion.

The elastic cotunneling processes that do not change the dot state or its energy allow for an electron exchange with the reservoirs via an intermediate virtual state. This leads to a finite linear conductance $G = dI/dV|_{V=0}$. The noise is also nonvanishing at zero bias, known from equilibrium fluctuation-dissipation theorem (FDT), $S = 4k_BTG$. In the Coulomb-blockade regime the FDT can be extended to nonequilibrium [14] and takes the form $S^{(2)}(V)/2eI^{(2)}(V) = \coth(eV/2k_BT)$. Our theory fulfills this relation; however, we stress that the FDT holds only in the regime of purely *elastic* cotunneling processes. In Fig. 2 we show the current I normalized to $\pi e\Gamma/h$ for the same set of energy parameters as in Fig. 1 but with a finite interaction $U = 4$ meV. Since the bias is applied symmetrically, the dot preferably occupies the state with spin $\downarrow$ (Coulomb blockade) until it can be emptied due to first-order hopping processes about 3 mV (first step). Further steps arise about 5 and 9 mV due to the double occupied dot state. This parameter set is similar to the experimental situation of Ref. [13] for a quantum dot with occupation $N = 2$ [19]. In Fig. 3 of that paper, a conductance feature (step) is observed inside the Coulomb-blockade diamond, which is attributed to the inelastic cotunneling processes. For our model one expects this inelastic cotunneling feature in the conductance at a bias of $\epsilon_{co}/e = (\epsilon_\uparrow - \epsilon_\downarrow)/e = 2$ mV. This feature is hardly noticeable in the conductance plot of the inset of Fig. 2, because our coupling Γ is relatively weak and the energy ϵ_{co} is fairly close to the sequential-tunneling energy. However, the inelastic cotunneling processes can be very clearly observed in the shot noise and the Fano factor $F = S/2eI$, as discussed below.

We note that the dashed and dotted curves in Fig. 2 with same total sum $(\Gamma + k_BT)$ almost lie on top of each other. The differential conductance plot (inset) shows that the

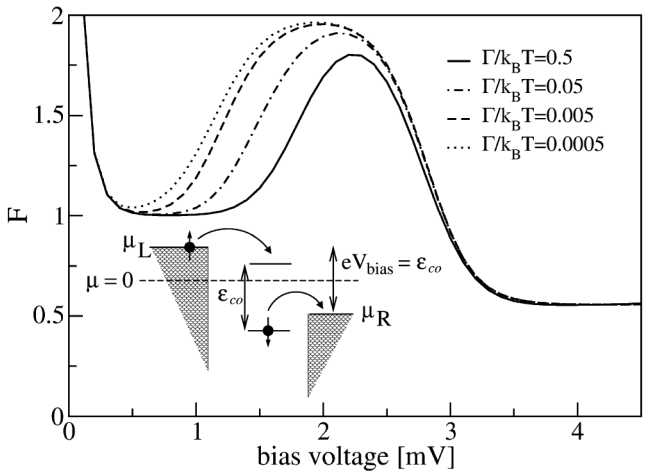

FIG. 3. The Fano factor $F = S/2eI$ vs bias voltage for the same parameter set as Fig. 2 but fixed temperature $k_BT = 0.1$ meV and various Γ. Inelastic cotunneling leads to a super-Poissonian Fano factor for biases around $\sim\epsilon_{co}/e = 2$ mV. First-order processes may also lead to a super-Poissonian value at a scale $\sim 2\epsilon_\uparrow/e = 1$ mV. The crossover between these energy scales runs over 3 orders of magnitude in the coupling. Outside the Coulomb-blockade regime the first-order results are recovered already at $\Gamma/k_BT \sim 0.1$. The inset shows a sketch of the transport situation at $eV_{bias} = \epsilon_{co}$.

temperature effect is a little stronger: the dashed curve with the highest temperature has the lowest peak. The full width of the conductance peaks is between 0.5–0.8 mV $\sim 6(\Gamma + k_B T)$, as compared to $5.44 k_B T$ for pure sequential tunneling [13]. The peak position shifts from the first-order value of 3 mV to lower bias, indicating the renormalization of the ''bare'' level.

The Fano factor $F = S/2eI$ for a fixed temperature and a sequence of coupling ratios $\Gamma/k_B T$ is shown in Fig. 3. At low bias, the Fano factor varies as [14] $\coth(eV/2k_B T)$ until it reaches the value 1, as expected for uncorrelated systems. For bias voltages around the spin-flip excitation energy $\epsilon_{co} = 2$ meV, the Fano factor becomes super-Poissonian [14], $F > 1$. Once sequential tunneling becomes dominant (at a bias ≥ 3 mV), the Fano factor drops to values between 1 and 1/2.

The super-Poissonian Fano factor appears for bias voltages at which the spin-$\uparrow$ level acquires some finite occupation probability. This can be either due to inelastic spin-flip cotunneling, appearing at a bias $\sim \epsilon_{co}/e = 2$ mV, or due to first-order tunneling processes [20] at a bias $\sim 2\epsilon_\uparrow/e = 1$ mV. The first-order processes are exponentially suppressed but, for the chosen parameters, still finite [20]. The enhancement of the noise comes from the second and third terms of Eq. (5), and, physically, is due to bunching of the transferred $\uparrow$ electrons during the time when this transport channel is not blocked by the dot being occupied with a $\downarrow$ electron. Both the position and the height of the peak in the Fano factor depends on all system parameters. In Fig. 3 we study the dependence on the ratio $\Gamma/k_B T$.

With increasing coupling strength Γ, the peak decreases and moves towards higher bias. For $\Gamma/k_B T = 0.0005$ our result (dotted line) coincides with that of a pure first-order calculation, which would show *no* dependence on $\Gamma/k_B T$ in this plot. However, at large coupling $\Gamma/k_B T = 0.5$ (solid line), the second order terms exceed the first-order contributions by several orders of magnitude in the Coulomb-blockade regime. Here, the cotunneling processes are only algebraically suppressed, compared to the exponential suppression of the sequential processes. Consequently, the elastic cotunneling processes wipe out the transport features due to purely sequential processes. Inelastic cotunneling, however, leads again to super-Poissonian shot noise of a magnitude that may be experimentally accessible [11] for the larger $\Gamma/k_B T$ values. We emphasize that, since the peak is close to the onset of sequential tunneling, a theory purely based on cotunneling processes [14] would not be sufficient. The importance of cotunneling processes for the Fano factor at rather weak coupling in the Coulomb-blockade regime contrasts with the situation at larger bias where second order corrections become noticeable only for $\Gamma/k_B T \sim 0.1$.

In summary, we presented a fully consistent theory of current and shot noise within a diagrammatic technique that includes higher-order tunneling processes in the coupling Γ of a quantum dot to metallic electrodes. As an example, we studied current and noise for an Anderson-impurity model with a finite spin splitting. We showed that especially the steps and the Coulomb-blockade regions are strongly affected by second order processes. Cotunneling processes dominate the sequential processes in the Coulomb-blockade regime and lead to super-Poissonian shot noise at the energy scale of inelastic cotunneling processes. With the experimental observation of such effects the characterization of quantum dots (or molecules) and their couplings to electrodes could be vastly improved.

We enjoyed interesting and helpful discussions with Jasmin Aghassi, Alessandro Braggio, Rosario Fazio, Göran Johansson, and Jan Martinek, as well as financial support by the DFG via the Center for Functional Nanostructures, SFB 491 and GRK 726.

[1] Ya. M. Blanter and M. Büttiker, Phys. Rep. **336**, 1 (2000).
[2] A. Thielmann, M. H. Hettler, J. König, and G. Schön, Phys. Rev. B **68**, 115105 (2003); **71**, 045341 (2005).
[3] S. Hershfield *et al.*, Phys. Rev. B **47**, 1967 (1993); A. N. Korotkov, *ibid.* **49**, 10 381 (1994); Yu. V. Nazarov and J. J. R. Struben, *ibid.* **53**, 15 466 (1996); G. Kiesslich *et al.*, Phys. Status Solidi C **0**, 1293 (2003).
[4] B. Elattari and S. A. Gurvitz, Phys. Lett. A **292**, 289 (2002).
[5] G. Michalek and B. R. Bulka, Eur. Phys. J. B **28**, 121 (2002).
[6] A. Mitra, I. Aleiner, and A. J. Millis, Phys. Rev. B **69**, 245302 (2004).
[7] B. R. Bulka, J. Martinek, G. Michalek, and J. Barnaś, Phys. Rev. B **60**, 12 246 (1999); A. Cottet, W. Belzig, and C. Bruder, Phys. Rev. Lett. **92**, 206801 (2004).
[8] S. Hershfield, Phys. Rev. B **46**, 7061 (1992); J. X. Zhu and A. V. Balatsky, Phys. Rev. B **67**, 165326 (2003); M. Hamasaki, *ibid.* **69**, 115313 (2004).
[9] H. Birk, M. J. M. de Jong, and C. Schönenberger, Phys. Rev. Lett. **75**, 1610 (1995).
[10] S. S. Safonov *et al.*, Phys. Rev. Lett. **91**, 136801 (2003).
[11] A. Nauen *et al.*, Phys. Rev. B **70**, 033305 (2004).
[12] D. V. Averin and A. A. Odintsov, Phys. Lett. A **140**, 251 (1989); D. V. Averin and Yu. V. Nazarov, Phys. Rev. Lett. **65**, 2446 (1990).
[13] S. De Franceschi *et al.*, Phys. Rev. Lett. **86**, 878 (2001).
[14] E. V. Sukhorukov, G. Burkard, and D. Loss, Phys. Rev. B **63**, 125315 (2001).
[15] J. König, H. Schoeller, and G. Schön, Phys. Rev. Lett. **76**, 1715 (1996); J. König, J. Schmid, H. Schoeller, and G. Schön, Phys. Rev. B **54**, 16 820 (1996).
[16] A. Braggio, J. König, and R. Fazio, cond-mat/0507527.
[17] M. H. Hettler, W. Wenzel, M. R. Wegewijs, and H. Schoeller, Phys. Rev. Lett. **90**, 076805 (2003).
[18] In systems with degeneracies not related to symmetries of the Hamiltonian, a generalization of our approach to off-diagonal density matrices might be necessary.
[19] Transport through a spin-split single-level Anderson model can be mapped onto a two-level Anderson model [2,5,7] for the temperature and bias range of interest.
[20] A. Cottet and W. Belzig, Europhys. Lett. **66**, 405 (2004).